

**Motor-driven effective temperature and viscoelastic response of active matter**Konstantin I. Morozov<sup>1</sup> and Len M. Pismen<sup>1,2</sup><sup>1</sup>*Department of Chemical Engineering, Technion–Israel Institute of Technology, Haifa 32000, Israel*<sup>2</sup>*Minerva Center for Nonlinear Physics of Complex Systems, Technion–Israel Institute of Technology, Haifa 32000, Israel*

(Received 17 March 2010; published 23 June 2010)

We consider dynamic response of a cytoskeletal network to both thermal and motor-induced fluctuations. The latter are viewed in two independent ways, as either additive or multiplicative colored noise. Due to a natural upper frequency limit of the motor agitation, the response of a living cell is similar to that of an equilibrium system in the high-frequency domain. At lower frequencies, the role of motor agitation manifests itself in intensified network fluctuations, which is equivalent to effective growth of the environment temperature. The effective temperature becomes frequency dependent, which signifies violation of the conventional fluctuation-dissipation theorem. The motor action affects the dynamic shear modulus in two opposite ways: by stiffening the network through filament prestress and softening it through increased agitation. The latter tendency is isolated when only single-headed motors are present. The theory is in good agreement with experimental measurements of the amplitude of the shear modulus under these conditions.

DOI: [10.1103/PhysRevE.81.061922](https://doi.org/10.1103/PhysRevE.81.061922)

PACS number(s): 87.10.Mn, 87.16.dj, 87.16.Ln, 05.40.–a

**I. INTRODUCTION**

The fluctuation-dissipation theorem (FDT) is one of the fundamental laws of equilibrium statistical mechanics. It establishes the connection between thermal fluctuations of some physical quantity and the response function describing variation of this quantity under the action of a weak external periodic field [1]. Violation of the FDT is always connected with nonequilibrium behavior of the system. Nevertheless, FDT has been extended [2] also to glasslike nonequilibrium systems by introducing some effective temperature  $T_{\text{eff}}$  differing from the thermodynamic temperature  $T$  of the system. The effective temperature in glasses and gels has been estimated both theoretically [3,4] and experimentally [5,6]. Some findings are, however, contradictory [5,6]. Moreover, it was found in a recent study of colloidal glasses, gels, and supercooled liquids [7] that the effective temperature  $T_{\text{eff}}$  coincided with the thermodynamic temperature, within the experimental accuracy, in the frequency range  $0.1-10^4$  Hz, so that no deviations from FDT were detected under these conditions.

The conventional FDT is certainly violated in biologically active systems, in particular, in living cells [8–12] where there is a source of agitation additional to thermal fluctuations. This activity is largely due to motor proteins converting chemical energy of adenosine triphosphate (ATP) molecules into mechanical work [13]. Theoretical description of the phenomenon is a formidable problem. As a rule, it is based on various kinds of specific models of filament-cytoplasm interactions [8,14,15]. In the present paper, we attempt to draw a general picture on a phenomenological level by computing the dynamic shear modulus  $G(\omega)$  of active matter and effective temperature under conditions of both thermal and motor activities. For this purpose, we generalize the approach by Gittes and MacKintosh [16] to semiflexible polymer networks subject to motor-driven fluctuations. The latter are introduced phenomenologically in two different ways: (i) as *additive* stochastic noise imitating active cytoplasmic stirring [17] or random motor binding-

unbinding processes and (ii) as *multiplicative* stochastic noise mimicking the active tension of the filaments. Both kinds of noise are motor driven and are present simultaneously. Nevertheless, in order to clarify the peculiarities of both mechanisms, we consider their action separately from each other.

The paper is organized as follows. In Sec. II, we reiterate main results of the well-established Granek-Morse-Gittes-MacKintosh (GMGM) theory of viscoelasticity of equilibrium semiflexible polymer networks [16,18,19] leading to the bending fluctuation spectrum and the response function, and check the relation between the two explicitly to facilitate further extension of the theory to nonequilibrium systems. In Sec. III, we generalize the classical problem to the case of motor activity and demonstrate the effect of additive colored motor noise. The case of multiplicative colored motor noise is studied in Sec. IV. In both cases, the results are given in terms of the effective frequency-dependent temperature  $T_{\text{eff}}(\omega)$ . It is shown that the natural upper frequency limit of motor agitation restores quasiequilibrium response at high frequencies. The effective temperature  $T_{\text{eff}}$  exceeds the thermodynamic temperature  $T$  only in the low-frequency domain where motor agitation prevails over thermal fluctuations. The dynamic shear modulus  $G(\omega)$  of active matter is computed and compared with available experimental data in Sec. V.

**II. VISCOELASTIC RESPONSE AT EQUILIBRIUM**

A network of cross-linked semiflexible polymers is characterized by a number of different length scales. A single filament is described by its contour length  $L$ , the steric diameter  $d$ , and the persistence length  $L_p = \kappa/T$ , where  $\kappa$  is the bending rigidity and  $T$  is the thermal energy (Boltzmann constant is rescaled to unity). An ensemble of filaments is characterized additionally by the mesh size  $\xi$  (the average distance between filaments) and by the entanglement length  $L_e$ , defined as a characteristic distance between polymer links, entanglement nodes, or other steric constraints. The abundance of length scales, which may be ordered in different

ways, leads to a wide variety of the various concentration regimes of semiflexible polymers [19]. The cytoskeletal actin filament network of living cells belongs to the class of tightly entangled polymers with the typical relation of length scales  $L \gg L_p \geq L_e \gg \xi \gg d$ .

Consider first a filament segment of length  $l \sim L_e$  stretched by a longitudinal force  $\tau$  under conditions of thermal equilibrium. The energy of the segment equals the sum of bending and stretching energies [19–21],

$$U = \frac{\kappa}{2} \int_0^l \left( \frac{\partial^2 \mathbf{y}}{\partial s^2} \right)^2 ds + \frac{\tau}{2} \int_0^l \left( \frac{\partial \mathbf{y}}{\partial s} \right)^2 ds, \quad (1)$$

where  $\mathbf{y}(s)$  is the transverse deviation of the segment and  $s$  is the arclength along its smooth averaged contour. The corresponding Langevin equation is

$$\zeta \partial \mathbf{y} / \partial t = -\kappa \partial^4 \mathbf{y} / \partial s^4 + \tau \partial^2 \mathbf{y} / \partial s^2 + \mathbf{f}(s, t), \quad (2)$$

where  $\zeta$  is the friction coefficient (per unit chain length) for transverse undulations of the polymer and  $\mathbf{f}(s, t)$  is a random force, assumed to be uncorrelated white noise with  $\langle f_\alpha(s, t) \rangle = 0$  and the correlation function

$$\langle f_\alpha(s, t) f_\beta(s', t') \rangle = 2T\zeta \delta_{\alpha\beta} \delta(s - s') \delta(t - t'). \quad (3)$$

The fluctuating quantity of interest in this formalism is the total end-to-end distance change of an inextensible segment,  $\delta l(t)$  [16,18]. For small deformations, it is defined as [21]

$$\delta l(t) = -\frac{1}{2} \int_0^l (\partial \mathbf{y} / \partial s)^2 ds. \quad (4)$$

In general, the variation  $\delta l(t)$  can be treated in two alternative ways. The first (active) technique determines the response of the projected length to an additional oscillating force  $\tau(\omega) \exp(-i\omega t)$ . The corresponding response function is  $\alpha(\omega) = \delta l(\omega) / \tau(\omega)$ . The second (passive) technique is based on computing the correlation function of the end-to-end thermal fluctuations,

$$\phi(t) = \langle \delta l(t) \delta l(0) \rangle - \langle \delta l(0) \rangle^2. \quad (5)$$

FDT establishes the relation between the imaginary part  $\alpha''(\omega)$  of the response function and the spectral density  $(\delta l^2)_\omega$ ,

$$\alpha''(\omega) = (\omega/2T)(\delta l^2)_\omega. \quad (6)$$

The advantage of the formalism based on Eqs. (2) and (3) is a possibility to determine separately in a closed form both the left- and right-hand sides of Eq. (6) and thereby to check FDT directly. This technique will further enable us to compute the effective temperature and detect deviations from FDT in a nonequilibrium system.

The transverse displacement of the segment  $\mathbf{y}(s)$  is presented in a standard way as a sum of bending modes,

$$\mathbf{y}(s, t) = 2 \sum_{n=1}^{\infty} \mathbf{y}_n(t) \sin \frac{\pi n s}{l}. \quad (7)$$

Using this in Eq. (2) reduces the Langevin equation to the spectral form

$$\partial \mathbf{y}_n / \partial t = -(\nu_b n^4 + \nu_\tau n^2) \mathbf{y}_n + \mathbf{f}_n(t) / \zeta, \quad (8)$$

where  $\nu_b = (\pi/l)^4 \kappa / \zeta$  and  $\nu_\tau = (\pi/l)^2 \tau / \zeta$  are characteristic relaxation rates, and

$$\mathbf{f}_n(t) = l^{-1} \int_0^l \mathbf{f}(s, t) \sin \frac{\pi n s}{l} ds. \quad (9)$$

Similar to Eq. (3), the spectral force modes  $\mathbf{f}_n(t)$  are uncorrelated random variables with zero mean  $\langle \mathbf{f}_n(t) \rangle = 0$  and the correlation function

$$\langle f_{n,\alpha}(t) f_{p,\beta}(t') \rangle = T \zeta l^{-1} \delta_{np} \delta_{\alpha\beta} \delta(t - t'). \quad (10)$$

The spectral representation of the length change  $\delta l(t)$  takes the form

$$\delta l(t) = -\pi^2 l^{-1} \sum_{n=1}^{\infty} n^2 \mathbf{y}_n^2(t). \quad (11)$$

The bending modes excited by the stochastic modes  $\mathbf{f}_n(t)$  are themselves stochastic variables with zero mean  $\langle \mathbf{y}_n(t) \rangle = 0$ . Their nontrivial even-power averages can be found by solving Eq. (8) subject to correlation (10) in a standard way [22] for both passive and active microrheology settings.

Using the *passive* technique, one studies *free* fluctuations  $\delta l(t)$ . The formal solution of the Langevin equation (8) is

$$\mathbf{y}_n(t) = \zeta^{-1} \int_{-\infty}^t \mathbf{f}_n(t') e^{-a_n(t-t')} dt', \quad (12)$$

where  $a_n = \nu_b n^4 + \nu_\tau n^2$ . Multiplying Eq. (12) by  $\mathbf{y}_n(0)$  and averaging with the help of Eq. (10) yields the time correlation function

$$\langle \mathbf{y}_n(t) \cdot \mathbf{y}_n(0) \rangle = T(\zeta l a_n)^{-1} e^{-a_n t}. \quad (13)$$

Correlations of higher orders are computed in a similar way, e.g., for any component  $u_n(t)$  of  $\mathbf{y}_n(t)$ , we have

$$\langle u_n^2(t) u_n^2(0) \rangle = \langle u_n^2(0) \rangle^2 + 2 \langle u_n(t) u_n(0) \rangle^2. \quad (14)$$

This relation demonstrates that the stochastic variables  $\mathbf{y}_n(t)$  excited by Gaussian white noise are Gaussian as well. The end-to-end fluctuation correlation function  $\phi(t)$  follows from Eqs. (5), (4), (7), (13), and (14),

$$\phi(t) = \frac{\pi^4 T^2}{l^4 \zeta^2} \sum_{n=1}^{\infty} \frac{n^4}{a_n^2} e^{-2a_n t}. \quad (15)$$

The Fourier transform of this relation determines the power spectrum of the end-to-end thermal fluctuations,

$$(\delta l^2)_\omega = \frac{4\pi^4 T^2}{l^4 \zeta^2} \sum_{n=1}^{\infty} \frac{n^4}{a_n(4a_n^2 + \omega^2)}. \quad (16)$$

The *active* technique assumes that, besides a constant force  $\tau_0$ , there is also an oscillating component  $\tau_\omega$ ,

$$\tau = \tau_0 + \tau_\omega e^{-i\omega t}. \quad (17)$$

The linear response  $\delta l_\omega$  of the filament length to the oscillating force is defined by the response function  $\alpha(\omega) = \delta l_\omega / \tau_\omega$ , which can be computed by averaging Eq. (11). Using Eq.

(17) in Eq. (12) and linearizing with respect to  $\tau_\omega$  yields, after integration,

$$\left. \frac{\partial \langle \mathbf{y}_n^2(t) \rangle}{\partial \tau_\omega} \right|_{\tau_\omega \rightarrow 0} = - \frac{2\pi^2 T}{l^3 \zeta^2 a_n} \frac{e^{-i\omega t}}{2a_n - i\omega}. \quad (18)$$

The resulting explicit relation for the response function is [16,18,19]

$$\alpha(\omega) = \frac{2\pi^4 T}{l^4 \zeta^2} \sum_{n=1}^{\infty} \frac{n^4}{a_n(2a_n - i\omega)}. \quad (19)$$

Thus, we have determined independently the response function  $\alpha(\omega)$  and the power spectrum of thermal fluctuation  $\delta l_\omega$ . Substituting both quantities into Eq. (6) proves that FDT is indeed fulfilled, as expected in the case of thermodynamic equilibrium.

### III. MOTORS AS ADDITIVE NOISE

The above approach is readily generalized to active motor-driven systems. To extend the theory to active media, we should first define a specific way of describing the motor activity. We will do it in two different ways to be described separately in the sequel.

First, in addition to a passive stochastic force  $f_\alpha(s, t)$  we consider an active fluctuating force  $f_\alpha^M(s, t)$ , assumed to be a random variable with zero mean independent of thermal fluctuations,

$$\langle f_\alpha^M(s, t) \rangle = \langle f_\alpha(s, t) f_\beta^M(s', t') \rangle = 0. \quad (20)$$

We choose the active force correlation in the form of *correlated* (colored) noise,

$$\langle f_\alpha^M(s, t) f_\beta^M(s', t') \rangle = \gamma \mu \zeta e^{-\gamma|t-t'|} \delta_{\alpha\beta} \delta(s-s'). \quad (21)$$

Here,  $\mu$  is the characteristic active energy analogous to the thermal energy  $T$  in Eq. (3). One can roughly estimate it as the energy of ATP hydrolysis; thus,  $\mu \sim 10T$  [13]. The inverse correlation decay time  $\gamma$  plays a role of a cutoff frequency typical of the motor work [13], implying that at frequencies higher than  $\gamma$  the motors become inactive. The frequency  $\gamma$  can be identified with the characteristic motor attachment or detachment time. Thus, the motor fluctuating force  $f_\alpha^M(s, t)$  is introduced into the Langevin equation (2) as *additive colored Gaussian noise* [23].

We consider first the simplest limiting case of infinite cutoff frequency,  $\gamma \rightarrow \infty$ . Then the fluctuating motor force reduces to  $\delta$ -correlated white noise similar to thermal fluctuations in Eq. (3). It is clear that in this particular case a system with motor agitation is isomorphic to a purely thermal system taken at some effective temperature. Indeed, direct calculation of the response function  $\alpha(\omega)$  and the fluctuation spectrum  $(\delta l^2)_\omega$  identical to that in Sec. II shows the effective temperature to be equal to  $T_{\text{eff}} = T + \mu$ . Evidently, the fluctuation-dissipation relation (6) should hold for the effective temperature  $T_{\text{eff}}$  rather than for the thermodynamic temperature  $T$ . Thus, in the case of white motor noise,  $T_{\text{eff}}$  reduces to a constant differing from  $T$  only by a fixed factor. In the general case of colored noise,  $T_{\text{eff}}$  should be, however,

frequency dependent and cannot be unequivocally expressed through the motor power.

Further on, we will determine  $T_{\text{eff}}$  using the relation proposed in Ref. [2],

$$T_{\text{eff}} = \frac{\omega(\delta l^2)_\omega}{2\alpha''(\omega)}. \quad (22)$$

At equilibrium,  $T_{\text{eff}}$  reduces to  $T$  since FDT must hold. For a nonequilibrium system, the ratio  $T_{\text{eff}}/T$  can be viewed as a measure of motor activity.

We return now to the colored motor noise problem defined by Eqs. (2) and (21). Transverse fluctuations of the filaments include both thermal and motor components  $\mathbf{y}_n^T, \mathbf{y}_n^M$  as additive contributions,

$$\mathbf{y}_n(t) = \mathbf{y}_n^T(t) + \mathbf{y}_n^M(t). \quad (23)$$

The motor correlation function  $\langle \mathbf{y}_n^M(t) \cdot \mathbf{y}_n^M(0) \rangle$  is determined similarly to Eq. (13) using Eqs. (12) and (21),

$$\langle \mathbf{y}_n^M(t) \cdot \mathbf{y}_n^M(0) \rangle = \frac{\mu}{\zeta l a_n} \psi(a_n) \frac{\gamma e^{-a_n t} - a_n e^{-\gamma t}}{\gamma - a_n}. \quad (24)$$

The function  $\psi(a_n) = \gamma / (\gamma + a_n)$  determines the relative impact of different modes on the agitation: modes with the relaxation rate much higher than the cutoff frequency  $\gamma$  are effectively frozen.

Due to the additivity of the motor noise and the linearity of the Langevin equation (2), the Gaussian character of filament fluctuations is preserved [22]. In particular, it is easy to check that Eq. (14) holds as well for the components of the total fluctuation (23). Respectively, the end-to-end fluctuation correlation (5) is computed as

$$\phi(t) = \pi^4 l^{-2} \sum_{n=1}^{\infty} n^4 [\langle \mathbf{y}_n^T(t) \cdot \mathbf{y}_n^T(0) \rangle + \langle \mathbf{y}_n^M(t) \cdot \mathbf{y}_n^M(0) \rangle]^2. \quad (25)$$

The explicit expression for the power spectrum  $(\delta l^2)_\omega$  of the end-to-end fluctuation can be found here by using Eqs. (13) and (24) and Fourier transforming the result.

The motor contribution  $\alpha^M(\omega)$  to the response function is additive to its thermal value (19) and is determined in the same way,

$$\alpha^M(\omega) = \frac{2\pi^4 \mu}{l^4 \zeta^2} \sum_{n=1}^{\infty} \frac{n^4 \psi(a_n) (\gamma + 2a_n - i\omega)}{a_n(2a_n - i\omega)(\gamma + a_n - i\omega)}. \quad (26)$$

It is clear that in the limiting case of thermal white noise,  $\gamma \rightarrow \infty$  and  $\mu \rightarrow T$ , so that Eq. (26) reduces to Eq. (19). At high frequencies,  $\omega/2\pi \gg \gamma, \nu_b, \nu_\tau$  the leading term in Eq. (26) is

$$\alpha^M(\omega) = \frac{2\pi^4 \mu}{l^4 \zeta^2} \frac{i}{\omega} \sum_{n=1}^{\infty} \frac{n^4}{a_n} \psi(a_n). \quad (27)$$

Higher terms decay as  $\omega^{-7/4}$ . The resulting scaling of the motor-driven contribution proportional to  $\omega^{-1}$  is different from the well-known scaling  $\alpha^T(\omega) \propto \omega^{-3/4}$  which follows from Eq. (19) for the equilibrium network [16,18,19].

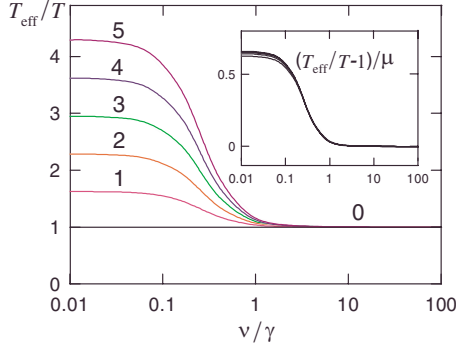


FIG. 1. (Color online) Effective temperature  $T_{\text{eff}}$  as a function of the dimensionless frequency  $\nu/\gamma$ , where  $\nu = \omega/2\pi$ , for chosen values of the dimensionless motor power  $\mu/T$ . The parameters are  $\nu_b/\gamma = 0.4$  and  $\nu_\tau/\gamma = 0.4$ . Inset: the function  $(T_{\text{eff}}/T - 1)/\mu$  plotted against  $\nu/\gamma$ .

Since both the response function  $\alpha(\omega)$  and the fluctuation spectrum  $(\delta l^2)_\omega$  are known, we can find the effective temperature  $T_{\text{eff}}(\omega)$  with the help of Eq. (22). The resulting ratio  $T_{\text{eff}}/T$  is plotted as a function of the dimensionless frequency  $\nu/\gamma = \omega/2\pi\gamma$  in Fig. 1 for several values of the dimensionless motor power  $\mu/T$ . We have used in the calculations the parameters of a real polymer network taken from Ref. [10]:  $\nu_b = 40$  Hz and  $\nu_\tau = 40$  Hz. The value of the cutoff frequency  $\gamma$  has been tentatively taken equal to 100 Hz. The conventional FDT is restored at  $\nu > \gamma$  since motors become inactive at high frequencies. Deviations from the conventional FDT increase with decreasing frequency and growing  $\mu$ . The curves for different  $\mu$ 's almost collapse to a single curve in the plot of the combination  $\mu^{-1}(T_{\text{eff}}/T - 1)$  shown in the inset.

Accounting for additive motor noise allows one to describe qualitatively recent experimental results by Mizuno *et al.* [10] measuring mechanical response of cross-linked actin filaments driven by myosin II molecular motors. Both measured spectra,  $\omega(\delta l^2)_\omega/2T$  and  $\alpha''(\omega)$ , are shown in Fig. 2 by the thin solid line and triangles, respectively. The theoretical dependences computed with the help of Eqs. (19), (26), and (25) are shown by the thick solid and dotted lines. We have

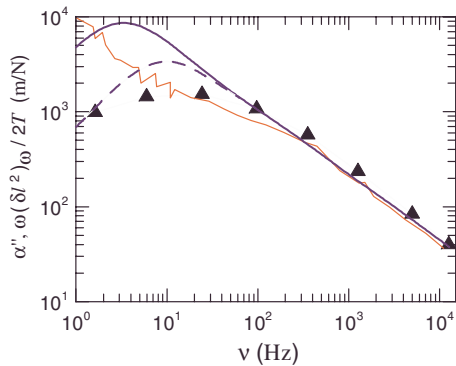


FIG. 2. (Color online) Comparison of the computed spectra  $\omega(\delta l^2)_\omega/2T$  (thick solid line) and  $\alpha''(\omega)$  (dashed line) for motor power  $\mu/T = 10$  with the respective experimental spectra [10] (shown, respectively, by the thin solid line and triangles). The parameters are  $\nu_b = \gamma = 20$  Hz and  $\nu_\tau = 40$  Hz.

used the values of parameters  $\nu_b = 20$  Hz and  $\nu_\tau = 40$  Hz close to those indicated in Ref. [10]. The motor power and cutoff frequency are taken to be  $\mu = 10T$  and  $\gamma = 20$  Hz, respectively. As seen in Fig. 2, the theoretical curves fit qualitatively the behavior observed in the experiment. In both cases, the spectra  $\omega(\delta l^2)_\omega/2T$  and  $\alpha''(\omega)$  are close to each other at high frequencies and notably different in the low-frequency domain where the motor-driven fluctuations prevail over thermal noise.

#### IV. MOTORS AS MULTIPLICATIVE NOISE

We return now to the Langevin equation (2) and switch on the motor activity in a different way, modeling it by a time-dependent stretching force  $\tau(t)$ . Accordingly, the motor fluctuating forces are introduced into the Langevin equation (2) as *multiplicative* white Gaussian noise [23]. The spectral equation (8) is now modified to

$$\partial \mathbf{y}_n / \partial t = -[\nu_b n^4 + \nu_\tau n^2 + \nu_m(t) n^2] \mathbf{y}_n + \mathbf{f}_n^T(t) / \zeta, \quad (28)$$

where  $\nu_m(t) = (\pi/l)^2 \tau_m(t) / \zeta$  and the parameters  $\nu_b$  and  $\nu_\tau$  are defined as before. The thermal origin of the additive noise  $\mathbf{f}_n^T(t)$  is indicated here explicitly.

As before, we start with the simplest case of  $\delta$ -correlated noise with zero mean,

$$\langle \tau_m(t) \rangle = 0, \quad \langle \tau_m(t) \tau_m(t') \rangle = 2J \delta(t - t'). \quad (29)$$

A rough estimate of the noise intensity  $J$  can be done according to Ref. [25].

The formal solution of Eq. (28) reads [cf. Eq. (12)]

$$\mathbf{y}_n(t) = \zeta^{-1} \int_{-\infty}^t \mathbf{f}_n^T(t') \exp \left[ -a_n(t - t') - n^2 \int_{t'}^t \nu_m(t_1) dt_1 \right] dt'. \quad (30)$$

Forming the quadratic functions and averaging them with the help of the expression

$$\left\langle \exp \left[ \int_0^t \epsilon(t_1) dt_1 \right] \right\rangle = \exp \left[ \frac{1}{2} \int_0^t \int_0^t \langle \epsilon(t_1) \epsilon(t_2) \rangle dt_1 dt_2 \right] \quad (31)$$

valid for a Gaussian process  $\epsilon(t)$  [23], we obtain

$$\langle \mathbf{y}_n(t) \cdot \mathbf{y}_n(0) \rangle = \frac{T}{\zeta l (a_n - 2a_n^M)} e^{-(a_n - a_n^M)t}, \quad (32)$$

where  $a_n^M = \nu_b n^4 = 2(\pi/l)^4 J n^4 / \zeta^2$ . Comparing this expression with its thermal analog (13) shows that multiplicative motor noise causes slowing down of the relaxational processes and increases the fluctuation amplitude. The fourth moment of any component  $u_n$  of the transverse fluctuation takes the form

$$\langle u_n^2(t) u_n^2(0) \rangle = \langle u_n^2 \rangle^2 \left[ 1 + 2 \frac{a_n - a_n^M}{a_n - 4a_n^M} e^{-2(a_n - 2a_n^M)t} \right]. \quad (33)$$

The discrepancy between this expression and Eq. (14) indicates a non-Gaussian character of bending fluctuations. The

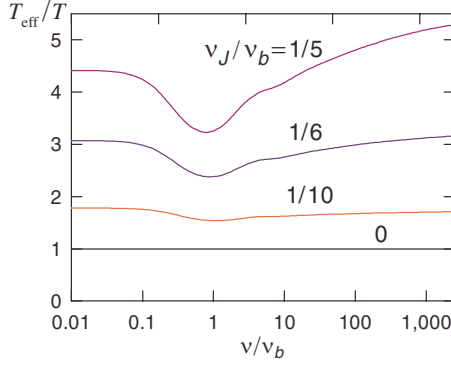


FIG. 3. (Color online) Effective temperature as a function of frequency for some values of the dimensionless motor activity  $\nu_J/\nu_b$  for the case of multiplicative white motor noise,  $\nu_\tau/\nu_b=1/4$ .

deviation can be quantified by calculating the kurtosis  $\Gamma_n(t) = \langle \Delta u_n(t)^4 \rangle / 3 \langle \Delta u_n(t)^2 \rangle$ , where  $\Delta u_n(t) = u_n(t) - u_n(0)$ . The analytical expression for  $\Gamma_n(t)$  is rather cumbersome. Its limiting values are  $\Gamma_n(0) = (1 - 2s_n)(1 - 13s_n^2) / [(1 - s_n)^2(1 - 4s_n)]$  and  $\Gamma_n(\infty) = (1 - 3s_n) / (1 - 4s_n)$ ;  $\Gamma_n(t)$  changes monotonically between these limits. The parameter  $s_n = a_n^M/a_n$  cannot exceed 1/4. Physically, this corresponds to failure of linear description by the Langevin equation in the form (2).

Next, we obtain the power spectrum of end-to-end fluctuations  $(\delta l^2)_\omega$  and the response function  $\alpha(\omega)$ . The former follows from Eqs. (11) and (33),

$$(\delta l^2)_\omega = \frac{4\pi^4 T^2}{l^4 \zeta^2} \sum_{n=1}^{\infty} \frac{1 - s_n}{(1 - 2s_n)(1 - 4s_n)a_n} \frac{n^4}{4a_n^2(1 - 2s_n)^2 + \omega^2}. \quad (34)$$

The response function is found analogously to Eqs. (17) and (18). In the case of motor activity, Eq. (18) remains valid with the substitution  $a_n \rightarrow a_n - a_n^M = a_n(1 - s_n)$ . Finally, the response function is computed as

$$\alpha(\omega) = \frac{2Tq^4}{\zeta^2} \sum_{n=1}^{\infty} \frac{n^4}{a_n(1 - s_n)[2a_n(1 - s_n) - i\omega]}. \quad (35)$$

The effective temperature determined from Eqs. (22), (34), and (35) for the dimensionless motor activity parameter  $\nu_J/\nu_b$  varying from zero to 1/5 and chosen values of prestress is plotted in Fig. 3. The dependence  $T_{\text{eff}}(\nu)$  is more complex than that for white additive noise where it reduces to a constant value but its frequency variation is not very pronounced. The effective temperature again increases with the noise intensity and, following a slight dip at  $\nu = O(\nu_b)$ , approaches a constant limit at high frequencies.

Finally, we consider a more general case of multiplicative colored noise with the correlation function

$$\langle \tau_m(t) \tau_m(t') \rangle = J \gamma e^{-\gamma|t-t'|}. \quad (36)$$

The effective temperature can be found numerically according to the scheme given above. We have used in calculations the same value  $\gamma = 100$  Hz of the cutoff frequency as before. The characteristic rates are taken as  $\nu_b = 40$  Hz and  $\nu_\tau = 10$  Hz, so that their ratio is the same as for the white noise

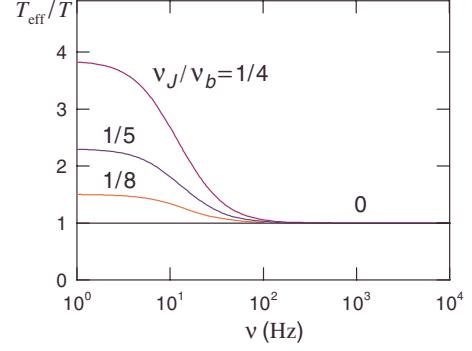


FIG. 4. (Color online) Effective temperature as a function of frequency for some values of the motor activity  $\omega_J$  for the case of colored motor noise. The parameters are  $\nu_b = 40$  Hz,  $\nu_\tau = 10$  Hz, and  $\gamma = 100$  Hz. The dimensionless value of motor activity  $\nu_J/\nu_b$  is indicated near the corresponding curve.

case in Fig. 3. The calculation results are shown in Fig. 4. The dependence of the effective temperature on frequency proves to be similar for both additive and multiplicative noise. The similarity of the results is not surprising since in both cases the spectrum of motor agitation has a natural upper limit—the cutoff frequency  $\gamma$ . At frequencies  $\nu > \gamma$ , the motors become inactive and only thermal fluctuation remains. Owing to the motors, the fluctuations become stronger and appear to be caused by environment temperature increasing over its thermodynamic value  $T$  to a frequency-dependent effective level  $T_{\text{eff}}$ . This can be viewed as violation of the conventional fluctuation-dissipation theorem expressed by Eq. (6).

## V. VISCOELASTIC RESPONSE OUT OF EQUILIBRIUM

The dynamic shear modulus  $G(\omega)$  of the network under conditions of both thermal and motor activities is proportional to the inverse to the response function  $\alpha(\omega)$  of a single filament [16,19],

$$G(\omega) = \chi \alpha^{-1}(\omega), \quad \chi = c \frac{LL_e}{15}. \quad (37)$$

The coefficient  $\chi$  is expressed here through the actin concentration  $c$ , the contour length  $L$ , and the entanglement length  $L_e$ ; the numerical factor has been obtained by averaging over random segment orientations. Below we will use instead an empirical value of this coefficient. The complex function  $G(\omega)$  can be represented in two equivalent forms,

$$G(\omega) = G'(\omega) - iG''(\omega) = |G(\omega)|e^{-i\delta(\omega)}, \quad (38)$$

which define the elastic (storage) modulus  $G'(\omega)$  and viscous (loss) modulus  $G''(\omega)$ , the amplitude  $|G|$ , and the phase angle  $\delta(\omega)$ .

The principal question is how the motors change viscoelastic properties of the actin network. Generally, the motor action affects  $G(\omega)$  in two opposite directions. On one hand, the motors are responsible for filament prestress. This leads to an increase in the shear modulus [10]. On the other hand, the motor agitation adds up to the thermal agitation

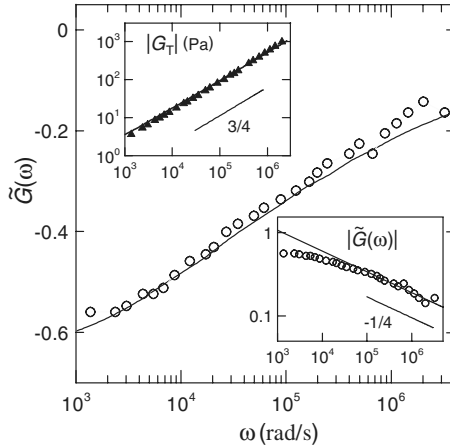


FIG. 5. The variation of the shear modulus amplitude  $\Delta|G(\omega)|$  of motor-driven network relative to its equilibrium value  $|G_T(\omega)|$ . Circles denote the data of Ref. [27]. The solid line is drawn using Eqs. (19), (26), and (37) with the parameters  $\nu_b=40$  Hz,  $\nu_r=0$ ,  $\gamma=1000$  Hz, and  $\mu/T=1.7$ . Upper inset: the amplitude of the shear modulus  $|G_T(\omega)|$  for an equilibrium system. The data (triangles) are taken from [27]. The solid line is a fit to the GMGM relation  $|G_T(\omega)| \sim \omega^{3/4}$  [16,18,19]. Lower inset: relative amplitude deviation  $\tilde{G}(\omega)$  [27] fitted to the  $\omega^{-1/4}$  asymptotic relation (straight line).

that reduces both elastic modulus and viscosity [26]. Both tendencies are, apparently, manifested simultaneously in the case of two-headed motors or motor groups [10,24]. The study of rheology of F-actin network in the presence of *single-headed* myosin motor protein by Goff *et al.* [27] is especially interesting in this regard. Single-headed myosin motors working in isolation do not contribute to prestress of actin filaments and, therefore, in accordance with the above reasoning, one may expect that the motor activity should soften the network. Indeed, the data of Ref. [27] clearly demonstrate a decrease in the viscoelastic modulus amplitude  $|G(\omega)|$  in the presence of motors by a factor of about 2, compared to its equilibrium value  $|G_T(\omega)|$  (see Fig. 5).

What kind of noise—additive or multiplicative—do single-headed motors produce? In general, both kinds of noise should be present also in this case. Indeed, according to Ref. [27], motor activity both generates a longitudinal mechanical force as a result of a power stroke and causes filament bending due to random binding and unbinding processes. The former produces multiplicative noise, whereas the latter is likely to generate additive noise. According to the estimates in Ref. [27], the duration of force production by a power stroke is much smaller than the characteristic time of myosin attachment. This indicates that network agitation is caused primarily by additive motor noise. We can use therefore Eq. (26) alongside with Eqs. (19) and (37), to fit the experimental data in Fig. 5. The equilibrium value has been fitted here to the GMGM relation  $|G_T(\omega)| \sim \omega^{3/4}$  [16,18,19] to obtain the coefficient  $\chi$  in Eq. (37) (see the upper inset in Fig. 5). The theoretical dependence calculated for the additive noise parameters  $\gamma=1000$  Hz and  $\mu/T=1.7$  proves to be in good agreement with the data [27].

We note that the empirical relation  $|G(\omega)| \sim \omega^{7/8}$  in Ref. [27] has to break down at high frequencies where the ratio

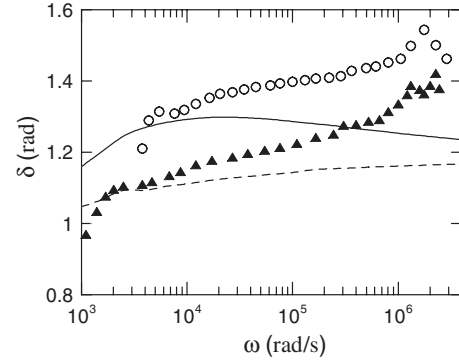


FIG. 6. The phase angle  $\delta(\omega)$  for equilibrium (dashed line) and active (solid line) networks. The experimental data are marked as in Fig. 5.

$|G_T|/|G|$  has to approach unity. A better motivated relation can be obtained for the relative deviation

$$\tilde{G}(\omega) = \frac{|G(\omega)|}{|G_T|} - 1. \quad (39)$$

The deviation decays asymptotically as  $\omega^{-1/4}$ , as seen in the lower inset in Fig. 5. This is in accordance with the  $\omega^{-1}$  decay of the motor-driven contribution to the response function  $\alpha(\omega)$  given by Eq. (27), which is faster than the  $\omega^{-3/4}$  decay of the contribution of thermal noise.

The exponent in the dependence  $G(\omega)$  differs from that calculated by Liverpool *et al.* [28]. The two results cannot be compared in view of a substantial difference between the models: Liverpool *et al.* [28] considered coupled longitudinal and transversal filament dynamics and assumed that the motor noise is white and affects the longitudinal motion only.

The behavior of the phase angle  $\delta(\omega)$  for both equilibrium and active networks is depicted in Fig. 6. The dashed line corresponds to the equilibrium GMGM theory. The solid curve for an active system has been computed using Eqs. (19), (26), and (37) with the same values of parameters as in Fig. 5. The theoretical results are in qualitative agreement with the data [27] but quantitative agreement is not as good as for the respective amplitudes in Fig. 5.

Up to now, we have studied the case of zero prestress of filaments. A stretching force exerted by two-headed motors or motor groups may lead to significant variations of elastic properties of the active system [14,20]. We demonstrate this by considering the storage  $G'(\omega)$  and loss  $G''(\omega)$  moduli of a stressed network under the action of additive colored motor noise. The values of the elastic modulus  $G'(\nu)$  normalized by its equilibrium low-frequency limiting value  $G_T(0)$  are drawn in Fig. 7 against the dimensionless frequency  $\nu/\nu_b$ . In the absence of motors,  $\mu=\nu_r=0$ , the function  $G'(\nu)$  (depicted by the dashed line in Fig. 7) reduces to its equilibrium GMGM form determined by Eqs. (19) and (37). The out-of-equilibrium curves (distinguished by the respective dimensionless prestress values) have been computed for a model case of additive colored motor noise with the power  $\mu/T=10$  and the cutoff frequency  $\gamma/\nu_b=25$ . We point out that motor activity *without* filament prestress leads to softening of the network (see the lower curve in Fig. 7), similar to the

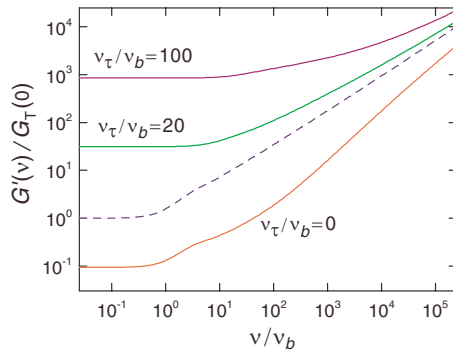


FIG. 7. (Color online) The elastic modulus  $G'(\nu)$  [normalized by its equilibrium low-frequency value  $G_T(0)$ ] as a function of the dimensionless frequency  $\nu/\nu_b$  for equilibrium (dashed line) and active (solid lines) networks. The parameters of additive colored noise are  $\mu/T=10$  and  $\gamma/\nu_b=25$ . The dimensionless values of the prestress  $\nu_\tau/\nu_b$  are indicated near the corresponding curves.

above case of single-headed myosin. The filament prestress causes widening of the plateau region and significant network stiffening in the low-frequency domain. For example, the stretching force with  $\nu_\tau/\nu_b=100$  gives rise to growth of the plateau elastic modulus by almost four orders of magnitude (see the upper curve in Fig. 7).

Let us estimate the corresponding dimensional value of the stretching force  $\tau$ . Since  $\nu_b=(\pi/l)^4\kappa/\zeta$  and  $\nu_\tau=(\pi/l)^2\tau/\zeta$ , we obtain for the actin network with the persistence length  $L_p\cong 17\ \mu\text{m}$  and the entanglement length  $l\cong 2\ \mu\text{m}$  [10] the value  $\tau\cong 20\ \text{pN}$ . This value is quite accessible for motors working collectively [10,13,24]. The above-mentioned variations of the elastic modulus  $G'$  in the low-frequency domain become, however, less pronounced with growing frequency. As seen in Fig. 7, all curves gradually approach the equilibrium curve  $G'_T(\nu)$ . This is another manifestation of weakening of motor activity in the high-frequency domain.

The corresponding frequency dependence of the loss modulus is shown in Fig. 8. The dependence follows approximately a power law at both low and high frequencies with an exponent changing close to the boundary of the elastic modulus plateau in Fig. 7. This is indicated by an ill-defined break of the slope in the log-log plot about this frequency, which becomes more pronounced at higher prestress.

## VI. CONCLUSION

The above phenomenological analysis of viscoelastic dynamic response of a semiflexible polymer network under

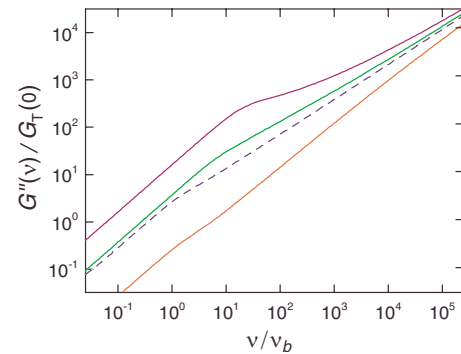


FIG. 8. (Color online) The loss modulus  $G''(\nu)$  [normalized by the equilibrium low-frequency value  $G_T(0)$  of elastic modulus] as a function of the dimensionless frequency  $\nu/\nu_b$  for equilibrium (dashed line) and active (solid lines) networks. The parameters and ordering of the curves are the same as in Fig. 7.

conditions of motor activity allows us to estimate effective temperature by computing separately in a closed form both the fluctuation correlation function and the spectral dynamic response. In contrast to near-equilibrium conditions when the conventional FDT is valid, the effective temperature is frequency dependent, being higher than thermodynamic temperature at low frequencies and going down to the thermodynamic value at frequencies exceeding the inverse characteristic time of motor activity. Motor agitation can act in two ways: as either additive or multiplicative colored noise. We have not detected qualitatively significant distinctions between the actions of additive and multiplicative noise, which, apparently, manifest themselves more prominently in the nonlinear regime.

The inverse correlation decay time of the colored noise  $\gamma$  determined by physical speed limitations of motor activity is the major factor governing the shape of all frequency dependences, but the effect is different for the effective temperature and viscoelastic response. The effective temperature quickly decays to its thermodynamic value at  $\nu > \gamma$ , but viscoelastic response only gradually approaches the near-equilibrium relation as the frequency grows following the  $\omega^{-1/4}$  asymptotic decay law.

## ACKNOWLEDGMENTS

This work was supported by the Human Frontier Science Program (Grant No. RGP0052/2009-C). K.I.M. acknowledges partial support by the Center of Absorption in Science, Ministry of Immigrant Absorption of Israel.

- [1] L. D. Landau and E. M. Lifshitz, *Statistical Physics Part 1* (Pergamon Press, Oxford, 1980).  
 [2] L. F. Cugliandolo, J. Kurchan, and L. Peliti, *Phys. Rev. E* **55**, 3898 (1997).  
 [3] L. F. Cugliandolo and J. Kurchan, *Phys. Rev. Lett.* **71**, 173 (1993).  
 [4] J. L. Barrat and W. Kob, *EPL* **46**, 637 (1999).

- [5] D. Bonn and W. K. Kegel, *J. Chem. Phys.* **118**, 2005 (2003).  
 [6] P. Wang, C. M. Song, and H. A. Makse, *Nat. Phys.* **2**, 526 (2006).  
 [7] S. Jabbari-Farouji, D. Mizuno, D. Derks, G. H. Wegdam, F. C. MacKintosh, C. F. Schmidt, and D. Bonn, *EPL* **84**, 20006 (2008).  
 [8] P. Martin, A. J. Hudspeth, and F. Jülicher, *Proc. Natl. Acad.*

- Sci. U.S.A.* **98**, 14380 (2001).
- [9] A. W. C. Lau, B. D. Hoffmann, A. Davies, J. C. Crocker, and T. C. Lubensky, *Phys. Rev. Lett.* **91**, 198101 (2003).
- [10] D. Mizuno, C. Tardin, C. F. Schmidt, and F. C. MacKintosh, *Science* **315**, 370 (2007).
- [11] D. Loi, S. Mossa, and L. F. Cugliandolo, *Phys. Rev. E* **77**, 051111 (2008).
- [12] F. Ziebert and I. S. Aranson, *Phys. Rev. E* **77**, 011918 (2008).
- [13] J. Howard, *Mechanics of Motor Proteins and the Cytoskeleton* (Sinauer, New York, 2000).
- [14] A. J. Levine and F. C. MacKintosh, *J. Phys. Chem. B* **113**, 3820 (2009).
- [15] N. Kikuchi, A. Ehrlicher, D. Koch, J. A. Käs, S. Ramaswamy, and M. Rao, *Proc. Natl. Acad. Sci. U.S.A.* **106**, 19776 (2009).
- [16] F. Gittes and F. C. MacKintosh, *Phys. Rev. E* **58**, R1241 (1998).
- [17] C. P. Brangwynne, G. H. Koenderink, F. C. MacKintosh, and D. A. Weitz, *Phys. Rev. Lett.* **100**, 118104 (2008).
- [18] R. Granek, *J. Phys. II* **7**, 1761 (1997).
- [19] D. C. Morse, *Macromolecules* **31**, 7030 (1998).
- [20] F. C. MacKintosh, J. Käs, and P. A. Janmey, *Phys. Rev. Lett.* **75**, 4425 (1995).
- [21] L. D. Landau and E. M. Lifshitz, *Theory of Elasticity* (Pergamon Press, Oxford, 1970).
- [22] M. Doi and S. F. Edwards, *The Theory of Polymer Dynamics* (Clarendon Press, Oxford, 1986).
- [23] H. Risken, *The Fokker-Planck Equation* (Springer, Berlin, 1989).
- [24] P.-Y. Plaçais, M. Balland, T. Guérin, J.-F. Joanny, and P. Martin, *Phys. Rev. Lett.* **103**, 158102 (2009).
- [25] B. Nadrowski, P. Martin, and F. Jülicher, *Proc. Natl. Acad. Sci. U.S.A.* **101**, 12195 (2004).
- [26] D. Humphrey, C. Duggan, D. Saha, D. Smith, and J. Käs, *Nature (London)* **416**, 413 (2002).
- [27] L. Le Goff, F. Amblard, and E. M. Furst, *Phys. Rev. Lett.* **88**, 018101 (2001).
- [28] T. B. Liverpool, A. C. Maggs, and A. Ajdari, *Phys. Rev. Lett.* **86**, 4171 (2001).